HHS Public Access

Author manuscript

Parkinsonism Relat Disord. Author manuscript; available in PMC 2021 July 01.

Published in final edited form as:

Parkinsonism Relat Disord. 2020 July ; 76: 21–28. doi:10.1016/j.parkreldis.2020.05.014.

Arterial spin labeling detects perfusion patterns related to motor symptoms in Parkinson's disease

Swati Rane, PhD[1], **Natalie Koh, BS**[1], **John Oakley, MD, PhD**[2], **Christina Caso, BS**[1], **Cyrus P. Zabetian, MD**[2,3], **Brenna Cholerton, PhD**[4], **Thomas J. Montine, MD, PhD**[4], **Thomas Grabowski, MD**[1]

[1]Integrated Brain Imaging Center, Radiology, University of Washington Medical Center, Seattle, WA

[2]Department of Neurology, University of Washington Medical Center, Seattle, WA

[3]Veterans Affairs Puget Sound Health Care System, Seattle, WA

[4]Department of Pathology, Stanford University, Stanford, CA 94305

INTRODUCTION

Parkinson's disease (PD) is a progressive movement disorder characterized by loss of dopaminergic neurons in the substantia nigra [1,2]. Loss of these neurons results in motor symptoms, including bradykinesia, rigidity, resting tremor, and postural instability. PD patients also show loss of cholinergic neurons, which further exacerbate cognitive symptoms [3]. Dopaminergic neurons are directly apposed onto microvasculature in the brain and alter local cerebral perfusion [4,5]. Similarly, cholinergic neurons are also known to modulate local vascular tone [6]. It is likely that cerebral blood flow (CBF) is altered due to neuronal degeneration and subsequent decrease in metabolic demands. Recent studies show posterior cortical hypoperfusion in PD participants compared to healthy older adults in posterior

Corresponding Author: Swati Rane, PhD, Integrated Brain Imaging Center, Radiology, University of Washington Medical Center, Seattle, WA 98195, Ph: 206 685 0457, srleven@uw.edu.

AUTHOR'S ROLES

Swati Rane: Conception, Organization, and Execution of research project, Design, and Execution of analyses methods for the study, design, and analyses of ASL data, manuscript writing

Natalie Koh: Study Coordinator for the MRI and SAI experiments, MDS-UPDRS, SAI data management, manuscript review, and critique

Christina Caso: Subject recruitment

Cyrus Zabetian: Subject recruitment and characterization, manuscript review and critique

Brenna Cholerton: Subject recruitment and characterization, manuscript review and critique

John Oakley: Design and analyses of SAI experiments, manuscript review and critique

Thomas Grabowski: Concept of research project and analysis methods, manuscript review and critique

Thomas Montine: Concept of research project, manuscript review and critique

Financial Disclosure/Conflict of Interest: None

FINANCIAL DISCLOSURES

Swati Rane, Natalie Koh, Thomas J Grabowski, Thomas Montine, Cyrus Zabetian, John Oakley, Brenna Cholerton: None

cingulate and parietal regions. Altered perfusion in PD is associated with cognitive symptoms, motor symptoms, and dopamine replacement therapy (DRT) [7,8].

Recently, using fluorodeoxyglucose (FDG) PET, studies identified PD-specific degeneration patterns of altered metabolism; a PD-related pattern (PDRP), associated with motor manifestations, and a PD-related cognitive pattern associated with cognitive impairments (PDCP) [9–11]. PDRP consists of the thalamus, pallidum, pons, motor cortex, lateral premotor and posterior parietal areas. PDCP consists of the dorsolateral prefrontal cortex, supplementary motor area, superior parietal regions, and cerebellum. MRI-derived CBF is an indirect marker of metabolism similar to FDG PET. Few studies have examined these patterns using ASL. Melzer et al. showed an ASL-PDRP pattern consisting of the parieto-occipital cortex, and precuneus, which was slightly different from the PET-derived PDRP pattern [12]. Teune et al. observed a similar PDRP pattern, including parieto-occipital cortex, anterior cingulate, thalamus, and motor regions[13]. While there were similarities between the PDRP patterns derived using ASL and PET, there are also differences attributable to variations in subject characteristics and imaging. The ASL-derived patterns still need to be confirmed.

Cholinergic dysfunction may contribute to PD symptoms, including motor manifestations, gait disturbances, olfactory, and sleep dysfunction [3,14–16]. It can adversely affect cognitive functions thereby, providing the basis for combination therapy to relieve PD symptoms [9,17,18]. One marker of cholinergic tone is transcranial magnetic stimulation (TMS), a non-invasive method to stimulate the brain[19]. When the primary motor cortex is stimulated with TMS, it activates the corticospinal pathway to generate a motor evoked potential (MEP) in the target muscle. At the same time, it also activates other inhibitory and excitatory circuits within the motor cortex. Afferent inhibition is the process by which a stimulus to sensory afferent nerves inhibits the contralateral motor neurons. Short latency afferent inhibition (SAI) refers to the inhibitory response (reduction of ~ 60-80% of the test MEP) to stimulus in about 20 ms [19–21].

Previous studies show that SAI response is normal in PD subjects in the OFF condition especially at the stimulus intervals of 20 ms [19]. Reduced amplitude of SAI, an indication of degree of inhibition, is typically demonstrable in the ON medication state [19]. In addition, to cholinergic pathways, SAI response is mediated by γ-aminobutyric acid (GABA) ergic pathways and by DRT. While the association between SAI and PD is unclear, the association between CBF and SAI response in PD is also underexplored. PD participants show CBF decreases in cholinergic targets such as the default mode, motor, and salience functional networks responsible for cognitive and motor symptoms in PD [24,25]. Moreover, SAI latency, which reflects conductance (speed of response), is relatively untested in PD [22,23].

We compared CBF in PD participants, ON, and 12 hours OFF their DRT using the Scaled Subprofile Modeling/Principal Component Analysis (SSM-PCA). Our goal was to replicate the PD-related abnormal perfusion networks reported by previous studies and subsequently evaluate how it changes with DRT. Ours is the first ASL study to evaluate PDRP modulation with DRT. We also measured SAI signal amplitude (ON state) and latency as a marker of

cholinergic deficit and determined the association between the SAI parameters and the PDRP pattern. We further evaluated the association of cognitive performance with the PDRP pattern and individual Principal Components (PCs).

METHODS

Subject selection.

Eighty-five individuals, including 26 controls (70±9 years, 11F) and 37 individuals with PD (67±8 years, 12F), were imaged per the Institutional Review Board and the Declaration of Helsinki for research involving human subjects. Individuals were diagnosed with PD during a consensus meeting following motor, cognitive, and neuropsychiatric assessments that included the Movement Disorders Society revision of the Unified Parkinson's Disease Rating Scale (MDS-UPDRS) Part III [26,27]. Other tests were the Montreal Cognitive Assessment (MoCA), Boston Naming Test (BNT), Symbol Digit Modality Test (SDT), and Logical Memory - immediate recall (LMI). All imaging was performed using a 3T Philips Achieva scanner (Best, Netherlands) and a 32-channel head coil with SENSitivity Encoding (SENSE) [28]. A second sample of 22 participants (6 control, 16 PD participants) imaged subsequently following the analysis of the above participants was set aside as a test set.

PD participants were scanned in the morning in the OFF state after withholding their DRT overnight. Then they took their DRT and were scanned again in the ON state after 90-120 minutes. The controls were scanned in one session. One control individual, receiving pro-cholinergic therapy, was excluded.

Measurements:

MRI—The T1 scan was performed in the OFF state. The parameters were: 3D MPRAGE sequence with a sagittal acquisition, resolution = 0.8 × 0.8 × 0.8 mm^3, repetition time (TR)/ echo time (TE) = 9.9/4.5 ms. Identical pCASL acquisition was performed in ON and OFF states. The parameters were: TR/TE = 5000/35 ms, 30 pairs of control and label images, resolution = 3.5 × 3.5 × 5 mm^3, background suppression (1710 ms, 2860 ms), label plane ~80 mm below the center of the imaging volume, labeling duration, τ, = 1800 ms and post labeling delay, ω, = 2000 ms[29]. Five averages of a reference M0 image were acquired with TR = 10000 ms. All other parameters were identical to the pCASL scan, but no labeling was performed.

Short-latency afferent inhibition (SAI).—To measure the cholinergic tone and its association with CBF, we performed SAI in the ON state in PD participants and controls. Afferent inputs were electrically activated to inhibit the contralateral motor cortex. Motor cortex was stimulated at intervals of 20 ms to inhibit the contralateral/affected side via the cholinergic and GABAergic pathways. Data collection was performed using LabChart 8 (AD Instruments, Sydney, AUS) and exported to Igor Pro (Wavemetrics, Tigurd, OR) for analyses. Conditioning median nerve stimulus was applied at 6 different inter-stimulus intervals, with 10 trials at each interval (N20 to N20+5). Twenty trials were conducted in the absence of the conditioning stimulus. The inter-stimulus interval (ISI) was determined based on the latency of the cortical N20 component of the somatosensory evoked potential.

Analyses:

CBF measurements.—Individual T1 images were registered to 2mm-MNI space in FSL v5.0 [30,31]. The ON and OFF scans were processed separately. The pCASL control and label images were registered using a modified realignment routine in SPM 12 [32] to account for the intensity fluctuations inherent in the ASL acquisition (higher signal intensity for control images alternating with lower signal intensity in label images). M0 images were registered and averaged together. Subsequently, the PCASL images were registered to the respective averaged M0 images. Difference maps (ΔM) were calculated and then registered to the segmented gray matter mask from the subject-specific T1 image and finally transformed to MNI space. This approach to registration using the difference map and segmented gray matter mask improves alignment and has been applied in the Genetic Frontotemporal dementia Initiative study [33]. Using the same transformations, the M0 image was registered to the MNI brain. The ΔM images were then divided by the M0 image, and CBF was calculated using the International Society for Magnetic Resonance in Medicine (ISMRM) recommendations [29]. A Quality Evaluation Index (QEI) was computed, and based on prior work comparing manual inspection, a QEI < 0.90 was considered to indicate poor quality (Supplementary data)[34]. Six participants were excluded based on the QEI.

SSM-PCA analyses.—The gray matter masks derived from the subject-specific T1 images were thresholded to include voxels with at least 35% gray matter. Previous studies have used a 10% threshold for gray matter and was considered too liberal for deriving a gray matter mask [13]. All gray matter masks were binarized and multiplied to obtain a common gray matter mask across all participants. The CBF maps were smoothed with a FWHM of 8 mm and multiplied by this mask. To account for partial volume effects, gray matter tissue probabilities were derived in SPM 12. The estimated CBF maps were divided by the gray matter tissue probability [35]. Data was log-transformed and de-meaned for each subject and group. Then, statistically independent PC images were calculated. The number of components was selected to account for 50% of the total variance. A generalized linear model using stepwise regression was applied to add or remove the selected PCs that separated normal healthy controls from PD participants using the Akaike Information Criterion (AIC, MATLAB command: stepwiseglm). As outlined by Meltzer et al. [12], the PDRP network was made using a linear combination of the retained PC images. The corresponding scores were also converted into a network score using the same linear combination. The PDRP network was standardized by subtracting the mean and dividing by the standard deviation of all voxels. The scores were also standardized. Further, the mean of just the control groups was subtracted from the standardized network Z-scores so that all expressions in the PD participants are deviations from the control group (Control PDRP score ~ 0). Then, the trained model from the stepwise regression was applied to new data (n = 22). The regression parameters used to identify the PDRP network from the training set were applied to this test set, similar to previous studies[13]. Receiver operating characteristic (ROC) curve and AUC were calculated for both training and test sets. Identical SSM-PCA procedures to those described above were performed to compared healthy controls and PD participants ON medication.

SAI amplitude and latency measurements.—Data from all trials was averaged and the signal amplitude was converted to a Z-score at each ISI. Since the study protocol only used 6 total time points, the complete N20 response peak (indicator of inhibition) and its return to baseline may not necessarily be captured. Therefore, a gaussian curve was fit to the data to identify the N20 peak and the latency (indicator of conductance speed) to the peak.

Association of CBF with motor impairment, SAI, and cognitive performance.—The PDRP network and the first few principal components that explained about 50% [12] of the variability in the data were considered for further analysis. For this association, all data from the training and validation sets were used together. The PCs on the validation set were obtained using the transformation matrices of the training set. The models to test were

$$\text{PRDP score/PC component} = (Age + Gender + Diagnosis) * X$$

where X = MDS-UPDRS motor scores, SAI amplitude, and SAI latency using R (v3.5) as well as MOCA, SDT, BNT, and LMI. The association with DRT measures in terms of levodopa equivalent dose (LED) [36] was tested only in the PD subgroup. Note that we use association to describe the effect i.e., test whether the beta coefficients of the above generalized linear model were significantly different from 0 or not. We use association in lieu of correlation.

RESULTS

Overall, the mean gray matter CBF in the control group (n=22) was 41±7 ml/100g/min, 42±8 ml/100g/min in the OFF state and 44±9 ml/100g/min in the ON state in PD group (n=35, disease duration = 10±5 years) . It was not different between groups after adjusting for age and gender. Table 1 outlines the demographics and average test scores for MDS-UPDRS, MOCA, BNT, SDT, and LMI. Average MDS-UPDRS motor scores were significantly different in the ON and OFF states (pairwise t-test, $p<0.001$) in the PD participants. All other scores were not significantly different between groups. SAI amplitude (Z) and latency (s) were not statistically different between groups. The LED in PD participants was 689±497 mg. Of the 22 controls, 9 individuals were cognitively impaired (clinical dementia rating, CDR=0.5) and of the 35 PD participants, 12 were cognitively impaired (CDR=0.5) and 5 had dementia (CDR=1).

SSM-PCA analysis - OFF.

In the OFF state, 6 PCs were identified to classify PD group from the controls on the training set. Of those, the PDRP network comprised of a linear combination of component 4 (β=0.16, p=0.001, explained variance, ev, =5.9%), and component 5 (β=0.07, p=0.04, ev=5.7%). The PDRP network is shown in Figure 1A. The PDRP included the posterior cingulate, precentral gyrus, precuneus, occipital fusiform gyrus, and sub-callosal cortex (fit p-value $<7.6e^{-5}$). Network Z-scores per group are shown in the bar graph. This network is similar to that identified by other studies [12,13]. The AUC curves for discriminating PD subject OFF medications from controls was 72% (**1B,** accuracy = 73.7%). In the test set, the AUC for discriminating PD subject OFF medications from controls was 71% (**1C,** accuracy

= 64%). The network score was significantly different between groups (**1D,** p=0.001) in the training set. The network scores from the test set show a similar difference (**1E**, p=0.01). The network scores were not associated with MDS-UPDRS, SAI, or neuropsychology battery, but only with diagnosis.

SSM-PCA analysis - ON.

In the ON state, the network comprised of only 1 component (PC 3, β=0.40, p=0.03, fit p=0.02) and included the posterior cingulate, precentral gyrus, precuneus, supplementary motor cortex, thalamus, occipital pole, and right hippocampus. The network is shown in Figure 2A. The network score was significantly different between groups (p=0.02). The PDRP network was not associated with SAI amplitude or latency. The AUC curves for discriminating PD subject ON medications from controls was 58% (**2B**, accuracy = 52%). In the test set, the AUC for discriminating PD subject ON medications from controls was 57% (**2C**, accuracy = 46%). These results indicate that CBF cannot distinguish PD participants ON medication from controls using the SSM PCA approach with PCs explaining 50% of the variance. The network score was significantly different between groups (**2D,** p=0.02) in the training set. The network scores from the test set show a similar difference (**2E**, p=0.01). The network scores were not associated with MDS-UPDRS, SAI, or neuropsychology battery but only with diagnosis.

Association with PD features and cognitive scores:

The first 6 components explaining 50% of the total variance in the OFF state (15.2%, 10.5%, 7.4%, 5.9%, 5.7% , and 4.6% respectively) and in the ON state (15.8%, 12.8%, 7.4%, 5.7%, 5.0% , and 4.3% respectively) are depicted in Figure 3A and B.

Association with PD features and cognitive performance.

Figures 4 and 5 show the association for the 6 PCs for all participants with diagnosis, SAI amplitude, SAI latency, UPDRS, MOCA, BNT, SDT, and LMI. In the OFF-condition, scores of PCs 4 and 5, which comprise the PRDP-network, expectedly show significant differences between controls and PD. PCs 2,3, and 4 were associated with UPDRS. PCs 1,3, and 4 were associated with SAI amplitude, and PCs 2 and 4 were associated with SAI latency. PCs 1,2, and 5 were associated with MOCA. Lastly, only PC2 was associated with BNT, SDT, and LMI.

In the ON state, PC3 scores were significantly different between controls and PD participants. This is expected since it represents the PDRP network in the ON state. MDS-UPDRS scores were associated with PCs 2 and 6. The association between both PC scores and UPDRS was modulated by age. No association was found with SAI amplitude. However, we found that PC4 and PC5 were associated with SAI latency PCs 3 and 6 were associated with MOCA, and PC4 and PC6 were associated with BNT.

DISCUSSION

Our work led to two major conclusions. First, a PD-related network PDRP can be well-detected using ASL in the OFF state. The ON state is thought to ‘normalize’ brain function,

and consistent with this, a disease-specific pattern of altered perfusion was not detected ON dopaminergic medication. Second, the related principal components (PCs) were associated with MDS-UPDRS scores, SAI measurements, as well as cognitive performance.

PDRP pattern detection.

Our study is the only one to our knowledge to show imaging data pre- and post DRT in the same participants using the SSM-PCA approach on ASL data. The study by Teune et al. included PD participants in whom DRT was stopped 12 hours prior, and benzodiazepines were stopped 24 hours before imaging, while in the study by Melzer et al., PD participants with and without DRT were combined.

We observed a PDRP network consisting of posterior cingulate, precentral gyrus, and the subcallosal cortex in the OFF state but not in the ON state. The regions of the PDRP network in the OFF state are similar to those observed by others [9,12,13]. There are some notable differences too. The PDRP network derived by Teune et al.[13] comprised of precuneus, posterior parietal, occipital, prefrontal, thalamus, pallidum, motor cortex, cerebellum, and the paracentral lobule. PDRP by Melzer et al. [12], comprised of posterior parietal region, precuneus, cuneus, and middle frontal gyrus. Variability in the networks could arise due to several factors. Unlike most previous studies, we separately calculated the PDRP network OFF and ON DRT. To confirm that PD patients OFF and ON DRT are not similar, we tested whether we could distinguish PD participants ON DRT using the PDRP network derived from the OFF state. The AUC was 39% (accuracy = 45%), indicating that PD participants ON medications could not be characterized by using the PDRP network derived in the OFF state in our study based on CBF.

A second reason that might account for differences among these studies is that image acquisition and processing were different across all three studies. The study by Teune et al. did not mention the ASL labeling parameters [13]. The study by Melzer et al. used a label duration and post labeling delay of 1500 ms [12], parameters recommended for young adult patients. Our study used a label duration of 1800 ms and post labeling duration of 2000 ms, which are in accordance with the recommendations by the ISMRM for performing pCASL acquisition in older adults with and without degenerative disease [29].

The PDRP examined using FDG PET did not differ in the ON and OFF medication states. Here, using ASL the pattern we see significant differences. Previous studies derived the PDRP pattern in all PD subjects (drug naive and OFF medication) together as one group, using considerably fewer subjects than ours [9,37]. As a consequence, the distinction between PDRP patterns in the ON and OFF status would be minimal by design. Additionally, although metabolism measurements using FDG and perfusion measurements using ASL are correlated with each other, their association may be altered in disease conditions. A recent study of FDG PET and ASL in the same participants with Lewy body disease showed that although very high, the ability of the two approaches to distinguish pathological brain from healthy brains is not identical. Interestingly, the patterns of hypometabolism and hypoperfusion were very similar in Lewy body disease [38]. Furthermore, DRT is known to alter the association between metabolism and perfusion [39].

While a PDCP network was not detected in this work, PC2 in the OFF-state was associated with UPDRS, MOCA, BNT, LMI, and SDT, i.e., all neuropsychological tests conducted in this study and could be analogous to the PDCP network. Similar to previous studies, PC2 included posterior cingulate, superior frontal gyrus, supplementary motor cortex regions.

Association with PD features and cognition.

Striatal dopamine release is modulated by cholinergic tone. SAI is thought to measure the cholinergic function in PD primarily due to dopaminergic-cholinergic imbalances. SAI amplitude and latency was associated with several principal components. The N20 latency was more variable in PD patients (0-6 s) than in controls (2-4 s), which might be due to either cholinergic dysfunction (OFF state) or DRT effects (ON state).

A PC decomposition is an excellent approach to visualizing CBF differences between groups. However, it is harder to interpret PCs. The positive (red) and negative (blue) saliences in an individual PC do not necessarily translate into absolute increases or decreases blood flow in the PD participants. For example, both $Z>2$ and $Z<-2$ regions in the PDRP OFF network (Supplementary Figure 3), show higher CBF in PD participants.

CONCLUSION

The PD-related pattern comprising of abnormal CBF in the precuneus, posterior cingulate, and subcallosal cortex distinguished the control participants from the PD participants in the OFF state. The PCs derived using SSM PCA were related to cognitive symptoms and cholinergic dysfunction as measured using SAI. Furthermore, the PDRP-related pattern was not distinguishable on the PD participants in the ON state. We believe that the ASL-based patterns of perfusion in PD have the potential to be suitable markers of motor symptom severity in PD. The clinical relevance of the study is that ASL is already a widely-available approach and is significantly cheaper than PET imaging. With, the SSM-PCA approach, ASL has not only the ability to discriminate PD patients from normal older adults but also monitor disease progression, and identify the efficacy of new treatments for PD.

Supplementary Material

Refer to Web version on PubMed Central for supplementary material.

ACKNOWLEDGEMENTS

This work was supported by Pacific Udall Center (2P50NS062684, PI: Montine, Project 2 PI: Grabowski), Dolsen Family Fund (PI: Swati Rane), K01AG055669 (NIH/NIA, PI: Rane). The authors thank Tim Wilbur and Serena Bennett, MRI technologists at the University of Washington, for scanning all participants and Krista Specketer for coordination of subject recruitment.

REFERENCES

[1]. Hammond C, Bergman H, Brown P, Pathological synchronization in Parkinson’s disease: networks, models and treatments, Trends Neurosci. 30 (2007) 357–364. [PubMed: 17532060]

[2]. Burn DJ, Rowan EN, Allan LM, Molloy S, O’Brien JT, McKeith IG, Motor subtype and cognitive decline in Parkinson’s disease, Parkinson’s disease with dementia, and dementia with Lewy

bodies, J. Neurol. Neurosurg. Psychiatry. 77 (2006) 585–589. 10.1136/jnnp.2005.081711. [PubMed: 16614017]

[3]. Bohnen NI, Albin RL, The cholinergic system and Parkinson disease, Behav. Brain Res. 221 (2011) 564–573. 10.1016/j.bbr.2009.12.048. [PubMed: 20060022]

[4]. Krimer LS, Iii ECM, Williams GV, Goldman-Rakic PS, Dopaminergic regulation of cerebral cortical microcirculation, Nat. Neurosci. 1 (1998) 286–289. 10.1038/1099. [PubMed: 10195161]

[5]. Kim KJ, Diaz JR, Iddings JA, Filosa JA, Vasculo-Neuronal Coupling: Retrograde Vascular Communication to Brain Neurons, J. Neurosci. 36 (2016) 12624–12639. 10.1523/JNEUROSCI.1300-16.2016. [PubMed: 27821575]

[6]. Amezcua JL, Palmer RMJ, de Souza BM, Moncada S, Nitric oxide synthesized from L-arginine regulates vascular tone in the coronary circulation of the rabbit, Br. J. Pharmacol. 97 (n.d.) 1119–1124. 10.1111/j.1476-5381.1989.tb12569.x.

[7]. Syrimi ZJ, Vojtisek L, Eliasova I, Viskova J, Svatkova A, Vanicek J, Rektorova I, Arterial spin labelling detects posterior cortical hypoperfusion in non-demented patients with Parkinson's disease, J. Neural Transm. Vienna Austria 1996. 124 (2017) 551–557. 10.1007/s00702-017-1703-1.

[8]. Barzgari A, Sojkova J, Maritza Dowling N, Pozorski V, Okonkwo OC, Starks EJ, Oh J, Thiesen F, Wey A, Nicholas CR, Johnson S, Gallagher CL, Arterial spin labeling reveals relationships between resting cerebral perfusion and motor learning in Parkinson's disease, Brain Imaging Behav. 13 (2019) 577–587. 10.1007/s11682-018-9877-1. [PubMed: 29744796]

[9]. Huang C, Mattis P, Tang C, Perrine K, Carbon M, Eidelberg D, Metabolic brain networks associated with cognitive function in Parkinson's disease, NeuroImage. 34 (2007) 714–723. 10.1016/j.neuroimage.2006.09.003. [PubMed: 17113310]

[10]. Poston KL, Eidelberg D, Functional brain networks and abnormal connectivity in the movement disorders, NeuroImage. 62 (2012) 2261–2270. 10.1016/j.neuroimage.2011.12.021. [PubMed: 22206967]

[11]. Ma Y, Tang C, Spetsieris PG, Dhawan V, Eidelberg D, Abnormal Metabolic Network Activity in Parkinson'S Disease: Test—Retest Reproducibility, J. Cereb. Blood Flow Metab. 27 (2007) 597–605. 10.1038/sj.jcbfm.9600358. [PubMed: 16804550]

[12]. Melzer TR, Watts R, MacAskill MR, Pearson JF, Rüeger S, Pitcher TL, Livingston L, Graham C, Keenan R, Shankaranarayanan A, Alsop DC, Dalrymple-Alford JC, Anderson TJ, Arterial spin labelling reveals an abnormal cerebral perfusion pattern in Parkinson's disease, Brain. 134 (2011) 845–855. 10.1093/brain/awq377. [PubMed: 21310726]

[13]. Teune LK, Renken RJ, de Jong BM, Willemsen AT, van Osch MJ, Roerdink JBTM, Dierckx RA, Leenders KL, Parkinson's disease-related perfusion and glucose metabolic brain patterns identified with PCASL-MRI and FDG-PET imaging, Neuroimage Clin. 5 (2014) 240–244. 10.1016/j.nicl.2014.06.007. [PubMed: 25068113]

[14]. Oh E, Park J, Youn J, Kim JS, Park S, Jang W, Olfactory dysfunction in early Parkinson's disease is associated with short latency afferent inhibition reflecting central cholinergic dysfunction, Clin. Neurophysiol. 128 (2017) 1061–1068. 10.1016/j.clinph.2017.03.011. [PubMed: 28400098]

[15]. Nardone R, Bergmann J, Brigo F, Christova M, Kunz A, Seidl M, Tezzon F, Trinka E, Golaszewski S, Functional evaluation of central cholinergic circuits in patients with Parkinson's disease and REM sleep behavior disorder: a TMS study, J. Neural Transm. 120 (2013) 413–422. 10.1007/s00702-012-0888-6. [PubMed: 22903350]

[16]. Lim Y, Ham J, Lee AY, Oh E, Gait Disturbance Associated with Cholinergic Dysfunction in Early Parkinson's Disease, J. Alzheimers Dis. Park. 7 (2017) 1–5. 10.4172/2161-0460.1000363.

[17]. Dubois B, Pillon B, Cognitive deficits in Parkinson's disease, J. Neurol. 244 (1996) 2–8. 10.1007/PL00007725.

[18]. Frucht S, Greene PE, An algorithm (decision tree) for the management of Parkinson's disease (2001): Treatment guidelines, Neurology. 58 (2002) 156–157. 10.1212/WNL58.L156.

[19]. Sailer A, Molnar GF, Paradiso G, Gunraj CA, Lang AE, Chen R, Short and long latency afferent inhibition in Parkinson's disease | Brain | Oxford Academic, Brain. 126 (2003) 1883–1894 [PubMed: 12805105]

[20]. Mancini M, Fling BW, Gendreau A, Lapidus J, Horak FB, Chung K, Nutt JG, Effect of augmenting cholinergic function on gait and balance, BMC Neurol. 15 (2015) 264 10.1186/s12883-015-0523-x. [PubMed: 26697847]

[21]. Ni Z, Chen R, Transcranial magnetic stimulation to understand pathophysiology and as potential treatment for neurodegenerative diseases, Transl. Neurodegener. 4 (2015) 22 10.1186/s40035-015-0045-x. [PubMed: 26579223]

[22]. Taylor JL, Burke D, Heywood J, Physiological evidence for a slow K+ conductance in human cutaneous afferents., J. Physiol. 453 (1992) 575–589. [PubMed: 1464845]

[23]. Bailey AZ, Asmussen MJ, Nelson AJ, Short-latency afferent inhibition determined by the sensory afferent volley, J. Neurophysiol. 116 (2016) 637–644. 10.1152/jn.00276.2016. [PubMed: 27226451]

[24]. Colloby SJ, McKeith IG, Burn DJ, Wyper DJ, O'brien JT, Taylor J-P, Cholinergic and perfusion brain networks in Parkinson disease dementia, Neurology. 87 (2016) 178–185. [PubMed: 27306636]

[25]. Hamel E, Cholinergic modulation of the cortical microvascular bed, in: Prog. Brain Res., Elsevier, 2004: pp. 171–178. 10.1016/S0079-6123(03)45012-7.

[26]. Goetz CG, Tilley BC, Shaftman SR, Stebbins GT, Fahn S, Martinez-Martin P, Poewe W, Sampaio C, Stern MB, Dodel R, Dubois B, Holloway R, Jankovic J, Kulisevsky J, Lang AE, Lees A, Leurgans S, LeWitt PA, Nyenhuis D, Olanow CW, Rascol O, Schrag A, Teresi JA, van Hilten JJ, LaPelle N, Movement Disorder Society-sponsored revision of the Unified Parkinson's Disease Rating Scale (MDS-UPDRS): Scale presentation and clinimetric testing results, Mov. Disord. 23 (2008) 2129–2170. 10.1002/mds.22340. [PubMed: 19025984]

[27]. Cholerton BA, Zabetian CP, Wan JY, Montine TJ, Quinn JF, Mata IF, Chung KA, Peterson A, Espay AJ, Revilla FJ, Devoto J, Watson GS, Hu S-C, Leverenz JB, Edwards KL, Evaluation of mild cognitive impairment subtypes in Parkinson's disease, Mov. Disord. 29 (2014) 756–764. 10.1002/mds.25875. [PubMed: 24710804]

[28]. Pruessmann KP, Weiger M, Scheidegger MB, Boesiger P, SENSE: sensitivity encoding for fast MRI, Magn. Reson. Med. 42 (1999) 952–962. [PubMed: 10542355]

[29]. Alsop DC, Detre JA, Golay X, Günther M, Hendrikse J, Hernandez-Garcia L, Lu H, Macintosh BJ, Parkes LM, Smits M, van Osch MJP, Wang DJJ, Wong EC, Zaharchuk G, Recommended implementation of arterial spin-labeled perfusion MRI for clinical applications: A consensus of the ISMRM perfusion study group and the European consortium for ASL in dementia, Magn. Reson. Med. 73 (2015) 102–116. 10.1002/mrm.25197. [PubMed: 24715426]

[30]. Jenkinson M, Beckmann CF, Behrens TEJ, Woolrich MW, Smith SM, FSL, Neuroimage. 62 (2012) 782–790. 10.1016/j.neuroimage.2011.09.015. [PubMed: 21979382]

[31]. Penny WD, Friston KJ, Ashburner JT, Kiebel SJ, Nichols TE, Statistical parametric mapping: the analysis of functional brain images, Elsevier, 2011.

[32]. Li Z, Douli S, Wang Z, Arterial Spin Labeling Perfusion MRI Signal Processing Toolbox (ASLtbx), (n.d.).

[33]. Mutsaerts HJMM, Petr J, Thomas DL, De Vita E, Cash DM, van Osch MJP, Golay X, Groot PFC, Ourselin S, van Swieten J, Laforce R, Tagliavini F, Borroni B, Galimberti D, Rowe JB, Graff C, Pizzini FB, Finger E, Sorbi S, Castelo Branco M, Rohrer JD, Masellis M, Macintosh BJ, GENFI investigators, Comparison of arterial spin labeling registration strategies in the multi-center GENetic frontotemporal dementia initiative (GENFI), J. Magn. Reson. Imaging JMRI. 47 (2018) 131–140. 10.1002/jmri.25751. [PubMed: 28480617]

[34]. Dolui S, Wolf R, Nabavizadeh SA, Wolk DA, Detre JA, Automated Quality Evaluation Index for 2D ASL CBF Maps, in: 22nd Annu. Conf., Hawaii, n.d.

[35]. Petr J, Mutsaerts HJMM, De Vita E, Steketee RME, Smits M, Nederveen AJ, Hofheinz F, van den Hoff J, Asllani I, Effects of systematic partial volume errors on the estimation of gray matter cerebral blood flow with arterial spin labeling MRI, Magma N. Y. N. 31 (2018) 725–734. 10.1007/s10334-018-0691-y.

[36]. Tomlinson CL, Stowe R, Patel S, Rick C, Gray R, Clarke CE, Systematic review of levodopa dose equivalency reporting in Parkinson's disease, Mov. Disord. Off. J. Mov. Disord. Soc. 25 (2010) 2649–2653. 10.1002/mds.23429.

[37]. Ko JH, Lerner RP, Eidelberg D, Effects of levodopa on regional cerebral metabolism and blood flow, Mov. Disord. 30 (2015) 54–63. 10.1002/mds.26041. [PubMed: 25296957]

[38]. Nedelska Z, Senjem ML, Przybelski SA, Lesnick TG, Lowe VJ, Boeve BF, Arani A, Vemuri P, Graff-Radford J, Ferman TJ, Jones DT, Savica R, Knopman DS, Petersen RC, Jack CR, Kantarci K, Regional cortical perfusion on arterial spin labeling MRI in dementia with Lewy bodies: Associations with clinical severity, glucose metabolism and tau PET, NeuroImage Clin. 19 (2018) 939–947. 10.1016/j.nicl.2018.06.020. [PubMed: 30003031]

[39]. Hirano S, Asanuma K, Ma Y, Tang C, Feigin A, Dhawan V, Carbon M, Eidelberg D, Dissociation of metabolic and neurovascular responses to levodopa in the treatment of Parkinson's disease, J. Neurosci. Off. J. Soc. Neurosci. 28 (2008) 4201–4209. 10.1523/JNEUROSCI.0582-08.2008.

Highlights

1. A Parkinson's disease related disease pattern was identified using ASL MRI and the Scaled Subprofile Modeling/Principal Component Analysis, which was capable of separating PD subjects (off medications) from the healthy older adults with an accuracy of 71%.
2. On medications, the PD subjects could not be reliably separated from the heathy older adults.
3. Principal components were associated with cognitive performance and MDS-UPDRS scores.

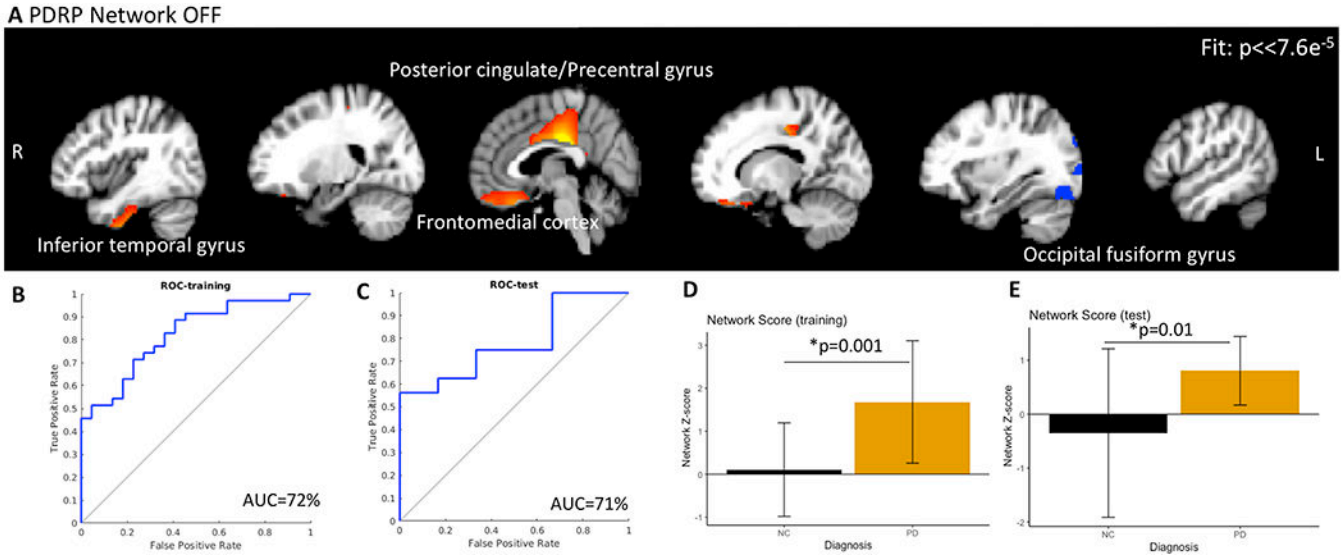

Figure 1.

(**A**) The PDRP network in the OFF condition and PDRP-network Z-scores. Closer the score to zero, more normal the individual. The PDRP network consisted of posterior cingulate, precuneus, subcallosal cortex (medial frontal), and occipital cortex. (**B, C**) represents the ROC plots for the training and test sets for distinguishing PD participants OFF medication from controls (AUC = 72.2%) and for distinguishing PD participants ON medication from controls (AUC = 71.0%). The network Z scores for both sets are shown in **D** and **E**. The network scores were significantly different between controls and PD.

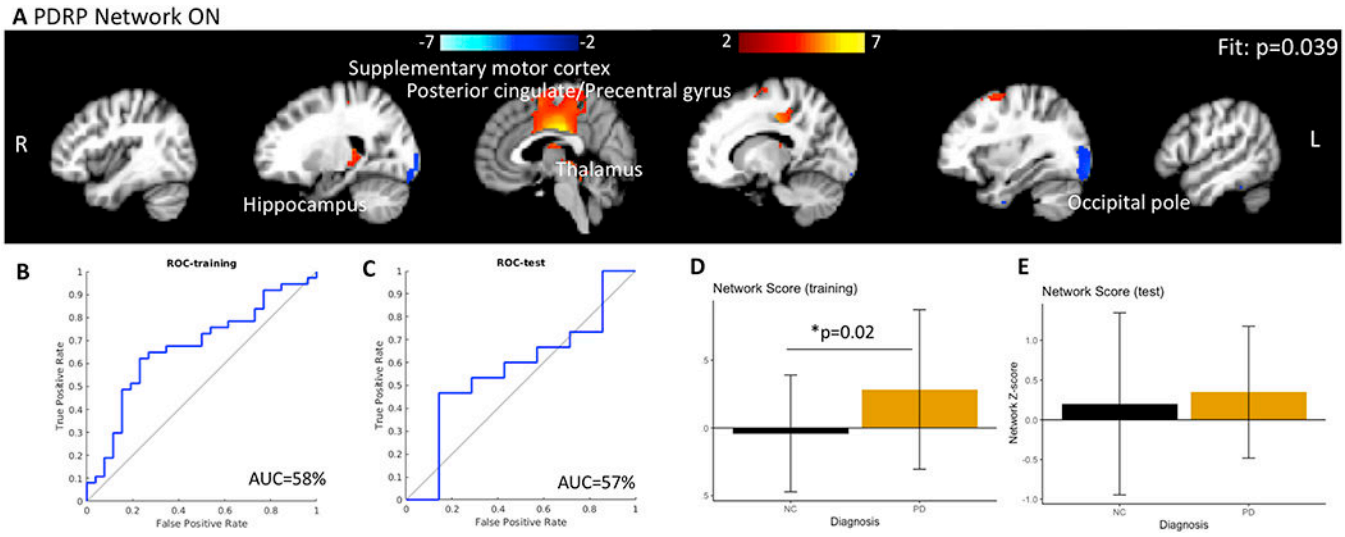

Figure 2.

(A) The PDRP network in the ON condition and PDRP-network Z-scores. Closer the score to zero, more normal the individual. The PDRP network in the ON state comprised of posterior cingulate, precuneus, and occipital cortex. No sub callosal cortex (medial frontal region) was identified. The distinction between the PDRP network scores, although significant, is less prominent in the ON condition than in the OFF condition. (**B, C**) represents the ROC plots for the training and test sets for distinguishing PD participants OFF medication from controls (AUC = 57.4%) and for distinguishing PD participants ON medication from controls (AUC = 45.1%). The network Z scores for both sets are shown in **D** and **E**. The network scores were marginally significantly different between controls and PD only in the training set.

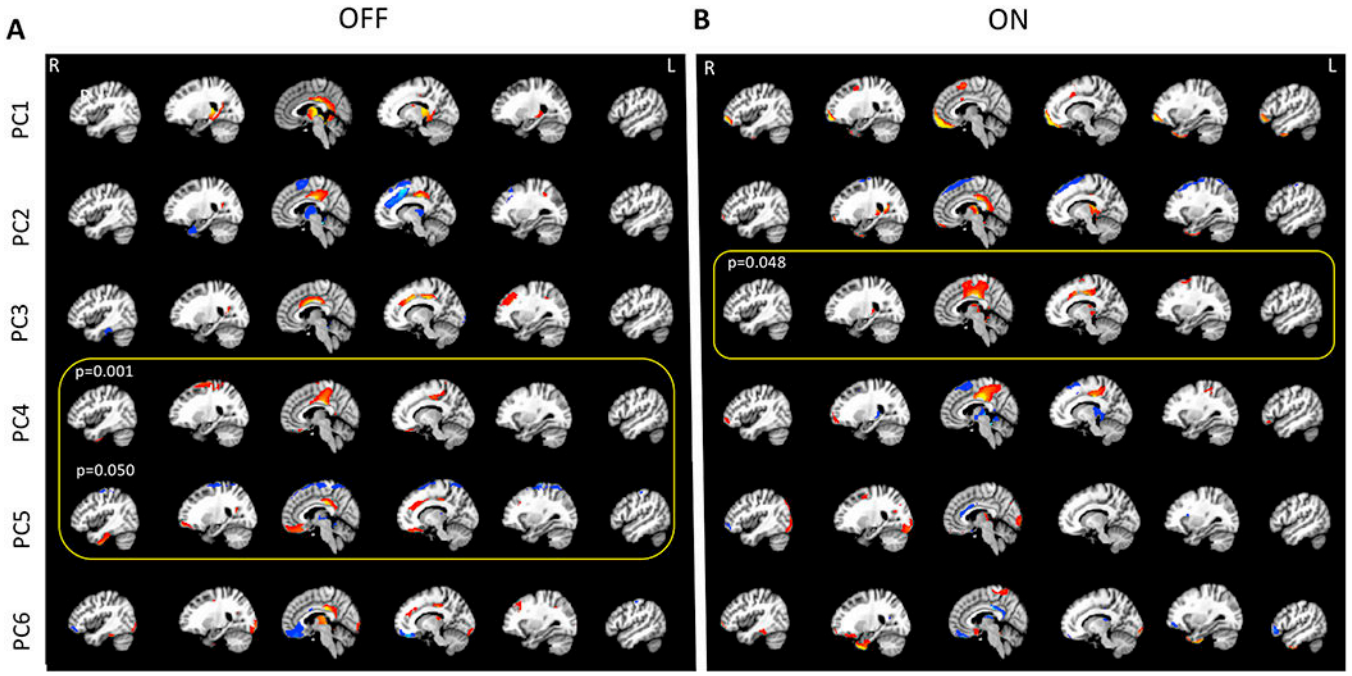

Figure 3.

(**A**) The first six PCs explaining about 50% of the variability in the data comparing control participants to PD subject OFF dopaminergic medication and (**B**) ON medication. In the OFF condition, PC1, explaining 15.2% of the variance, comprised of posterior cingulate, precuneus, thalamus, caudate, and cerebellum. PC2 explained 10.5% of the variance and included posterior cingulate, superior frontal gyrus, and the supplementary motor cortex. PC3 (explained variance 7.4%) included posterior cingulate, anterior cingulate, L middle frontal gyrus, while PC 4 (explained variance = 5.9%) comprised of posterior cingulate, postcentral gyrus, precentral gyrus, superior frontal gyrus, frontomedial cortex/subcallosal cortex, L occipital cortex. PC5 and PC6 explained 5.7 and 4.6% of the variance. PC5 included posterior cingulate, superior frontal gyrus, frontomedial cortex/subcallosal cortex, precentral gyrus and supplementary motor cortex, and PC6 included posterior cingulate, cuneus, bilateral temporo-occipital regions. In the ON state, PC1, explaining 15.8% of the variance, comprised of the frontal pole, supplementary motors cortex, and parahippocampal gyrus. PC2 explained 12.8% of the variance and included frontal pole, thalamus, parahippocampal gyrus, and the posterior cingulate. PC3 (explained variance 7.4%) included posterior cingulate, precentral gyrus, supplementary motor cortex, while PC 4 (explained variance = 5.7%) comprised of posterior cingulate, R frontal pole, and thalamus. PC5 and PC6 explained 5.0 and 4.3% of the variance. PC5 included Thalamus and R occipital cortex. PC6 included postcentral gyrus, precentral gyrus, frontomedial cortex/subcallosal cortex, and temporo-occipital regions.

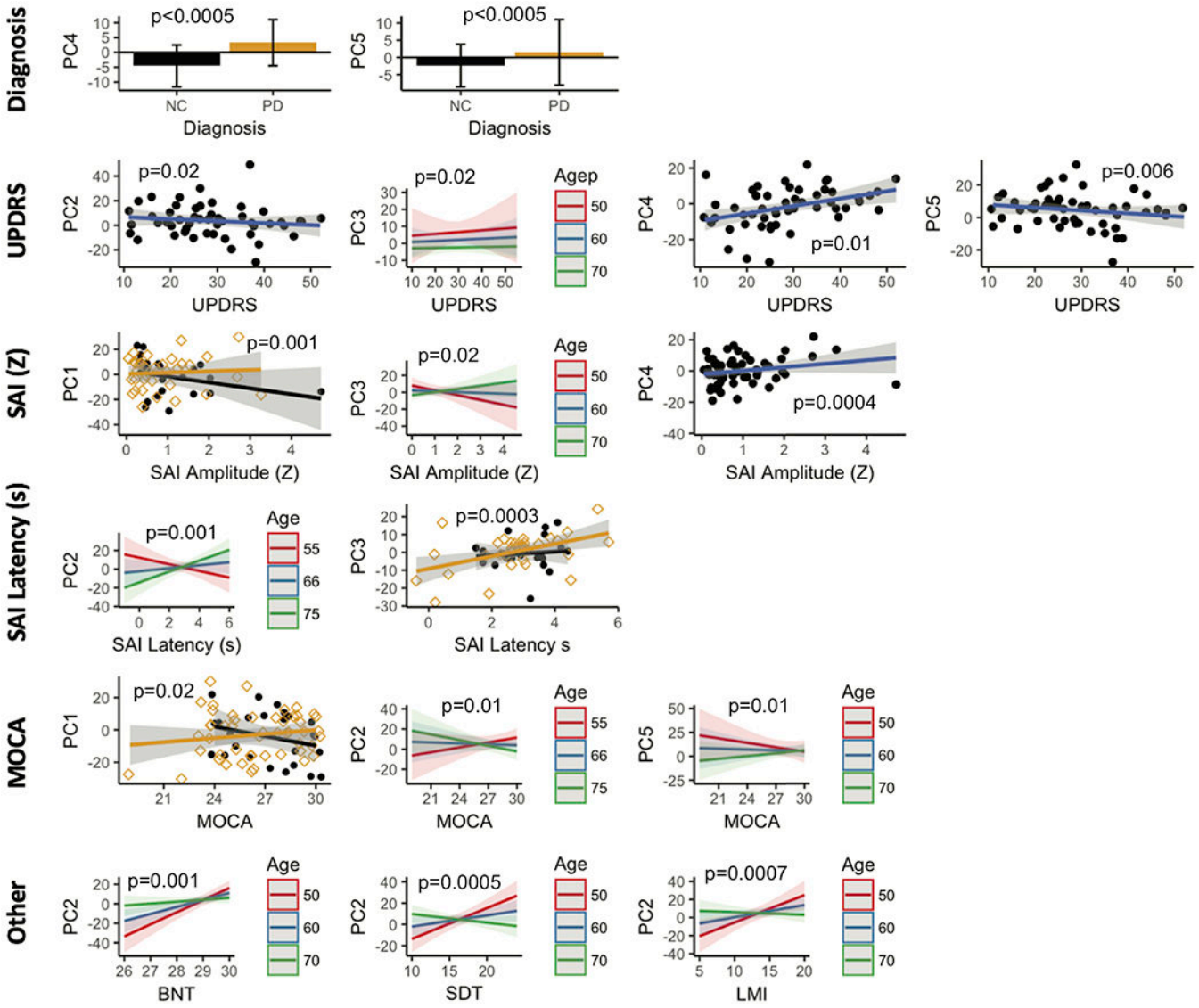

Figure 4.

The PCs in the OFF condition were tested for association with diagnosis, MDS-UPDRS, SAI measures, and cognitive performance while adjusting for age and gender. PC 4 and PC 5 contributed to the PDRP network in the OFF state. PC 4 significantly ($p<0.0005$) discriminated controls form PD participants in the OFF condition. PC 5 was strongly associated with age ($p=0.003$). Lower PC 2 and PC 5 scores were associated with high MDS-UPDRs scores (PC 2, $p= 0.02$; PC5, $p = 0.006$). PC 4 showed the opposite trend ($p =0.01$). While high PC 3 scores were associated with high UPDRS scores, they decreased with age ($p = 0.02$). Higher PC 1 scores were associated with low SAI amplitude only in PD participants ($p = 0.001$). This relationship was observed for all participants for PC 3 but decreased with age ($p = 0.02$). Higher PC4 scores were associated with higher SAI amplitude ($p = 0.0004$). Lower PC 2 scores were associated with SAI latency, with this relationship reversing with increasing age ($p = 0.0001$). Lower PC 3 scores were associated with shorter latency times on SAI in controls only ($p = 0.003$). PC 1 showed opposite

correlations with MOCA scores (p = 0.03). Higher PC 2 scores were associated with higher MOCA scores, but this relationship reversed with age(p = 0.01). The exact opposite behavior was observed with PC 5 (p = 0.01). BNT, SDT, and LMI scores were all positively correlated with PC 2. This correlation reduced or even reversed with age in all tests. (p-value; BNT = 0.001, SDT <0.0005, LMI = 0.0007).

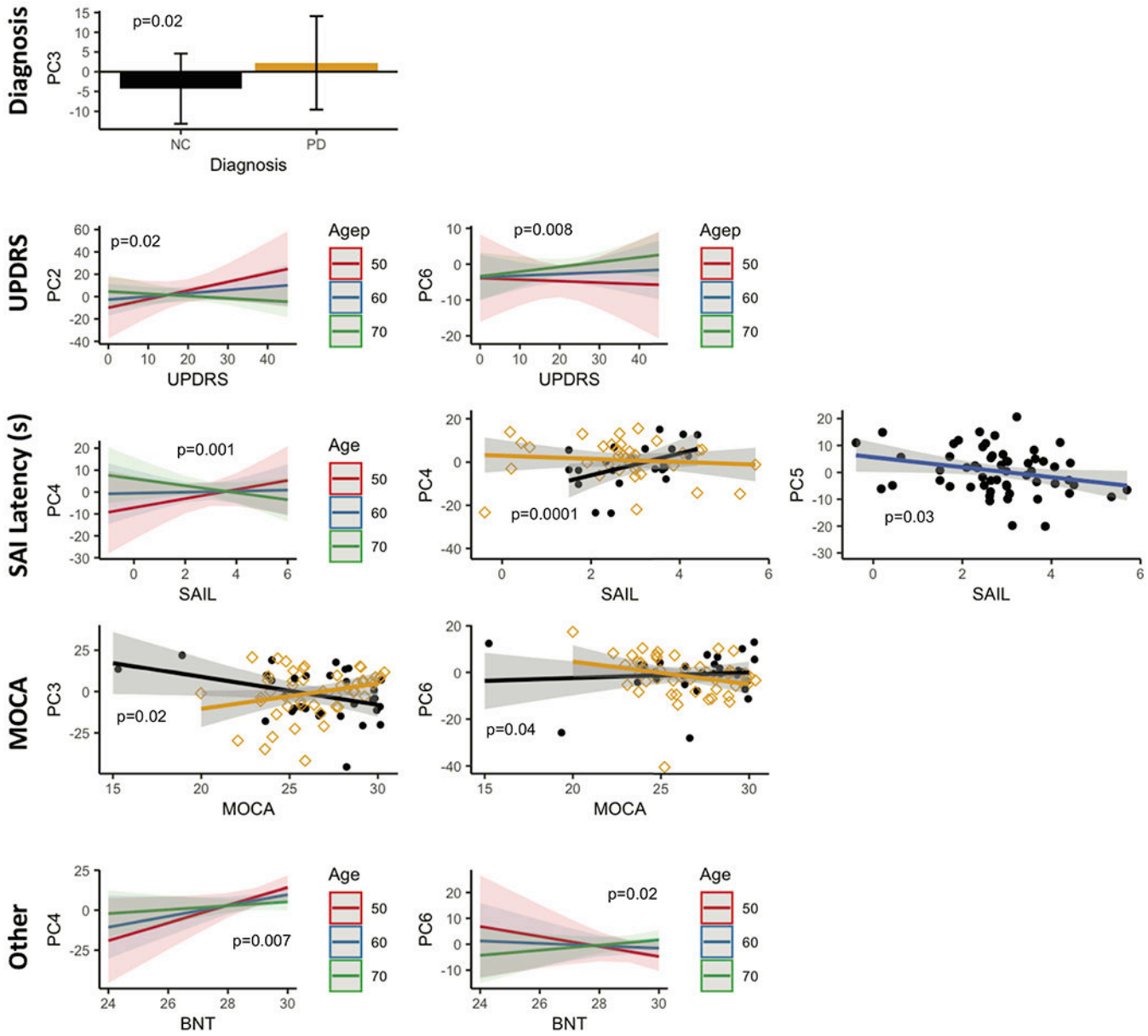

Figure 5.

The PCs in the ON condition were tested for association with diagnosis, MDS-UPDRS, SAI measures and cognitive performance while adjusting for age and gender. PC 3 scores were significantly different between controls and PD participants (p = 0.02). Higher UPDRs scores were associated with higher PC 2 scores. This correlation decreased with age (p =0.02). On the other hand, PC 6 correlations to UPDRS scores increased with age (p = 0.008). High PC 4 scores were correlated with high latency time for SAI, especially in controls (p = 0.001), and this correlation decreased, even reversed with age (p = 0.0001). High PC 5 scores were correlated with shorter latency on SAI irrespective of diagnosis (p = 0.03). While PC 3 scores showed a negative correlation with MOCA scores in PD participants (p = 0.02), PC 6 showed similar trends in controls (p = 0.04). Higher BNT scores were associated with higher PC 4 scores (p = 0.007) and lower PC 6 scores (p =

0.02). Both relationships were modulated by age. Note that the neuropsychological battery was conducted only once in the ON condition within 6 months of the imaging.

Table 1:

Subject Demographics

Description	Controls	PD	p-value
N	28	57	
Age (year)	69±8	67±8	
Gender	15M	33M	
MDS-UPDRS -OFF	3±10	28±10	
MDS-UPDRS -ON		21±8	
MOCA	27±2	26±2	*p<0.0001 between ON and OFF
BNT	29±1	29±1	
SDT	16±2	16±4	
LMI	13±3	13±4	
SAI Amplitude (Z)	1.08±0.99	0.88±0.80	
SAI Latency (s)	2.96±0.91	2.73±1.36	